

Biotin–Streptavidin-Induced Aggregation of Gold Nanorods: Tuning Rod–Rod Orientation

Anand Gole and Catherine J. Murphy*

Department of Chemistry and Biochemistry, University of South Carolina,
Columbia, South Carolina 29208

Received May 12, 2005. In Final Form: August 23, 2005

We report herein biotin–streptavidin-mediated aggregation studies of long gold nanorods. We have previously demonstrated end-to-end linkages of gold nanorods driven by the biotin–streptavidin interaction (Caswell et al. *J. Am. Chem. Soc.* **2003**, *125*, 13914). In that report, the specific binding of biotin disulfide to the gold nanorod edges was achieved due to the preferred binding of thiol molecules to the Au{111} surface (gold nanorod ends) as opposed to the gold nanorod side faces. This led to the end–end linkage of gold nanorods upon subsequent addition of streptavidin. In this report we demonstrate a simple procedure to biotinylate the entire gold nanorod surface and subsequently form a 3-D assembly by addition of streptavidin. Gold nanorods were synthesized by the three-step seeding protocol documented in our previous articles. The surface of gold nanorods was further modified by a layer of a weak polyelectrolyte, poly(acrylic acid), PAA. A biotin molecule which has an amine group at one end (biotin–PEO–amine) was anchored to the carboxylic acid group of the polyelectrolyte using the well-known carbodiimide chemistry. This process biotinylates the entire gold nanorod surface. Addition of streptavidin further leads to aggregation of gold nanorods. A closer look at the aggregates reveals a preferential side-to-side assembly of gold nanorods. The gold nanorods were characterized at each stage by UV–vis spectroscopy, light scattering, and transmission electron microscopy (TEM) measurements.

Introduction

It is well-known that individual nanoparticles have interesting properties that are different from those of the bulk.¹ Exciting properties emerge when these individual nanoparticles form a 2-D or a 3-D assembly.² The ability to tailor the separation of individual nanoparticles in this assembly, leading to tunable optoelectronic properties of the aggregate, is of great interest and a great challenge. Various efforts have been made to design suitable techniques to organize nanoparticles into 2-D³ or 3-D^{2,4} assemblies. Such assemblies are possible via self-assembly procedures governed by the surface chemistry of individual particles. This chemistry takes advantage of covalent or

noncovalent (antigen–antibody, electrostatic, hydrogen-bonding) interactions.^{3,4} Thus, knowledge of molecules on the surface is critical. By appropriate choice of capping agents, one could use nanoparticles for different applications such as solution-based sensors,⁵ nanoparticle thin films using particle–2-D-surface interactions,³ carrying out chemical reactions on surfaces, and so forth.⁶ If biomolecules such as proteins or DNA are used for surface modification, then nanoparticles could be used for bio-specific assays.⁷

While the controlled assembly of spherical nanoparticles in solution has met with a fair degree of success, 3-D assembly of other shapes such as nanorods and nanowires is less well-known.^{8,9} These studies use either specific (antigen–antibody)⁸ or weak secondary interactions.⁹ Mann and co-workers have shown that DNA-modified gold nanorods can be assembled into 3-D aggregates by the addition of a complementary linker DNA.^{8a} Mallouk and co-workers have assembled DNA-modified gold nanowires onto 2-D surfaces.^{8b} Chang et al. use the specific affinity of anti-mouse IgG toward mouse IgG to achieve oriented assembly of short gold nanorods in solution.^{8c} The use of

* Corresponding author. E-mail: murphy@mail.chem.sc.edu.

(1) (a) El-Sayed, M. A. *Acc. Chem. Res.* **2001**, *34*, 257; (b) A general review on gold nanoparticles: Daniel, M. C.; Astruc, D. *Chem. Rev.* **2004**, *104*, 293.

(2) (a) Weller, H. *Angew. Chem., Int. Ed. Engl.* **1996**, *35*, 1079; (b) Storhoff, J. J.; Lazarides, A. A.; Mirkin, C. A.; Letsinger, R. L.; Mucic, R. C.; Schatz, G. C. *J. Am. Chem. Soc.* **2000**, *122*, 4640; (c) Courtney, A.; Mermet, A.; Albouy, P. A.; Duval, E.; Pileni, M. P. *Nat. Mater.* **2005**, *4*, 395.

(3) (a) Brust, M.; Walker, M.; Bethell, D.; Schiffrin, D. J.; Whyman, R. *Chem. Commun.* **1994**, 801; (b) Colvin, V. L.; Goldstein, A. N.; Alivisatos, A. P. *J. Am. Chem. Soc.* **1992**, *114*, 5221; (c) Gole, A.; Sainkar, S. R.; Sastry, M. *Chem. Mater.* **2000**, *12*, 1234; (d) Gole, A.; Orendorff, C. J.; Murphy, C. J. *Langmuir* **2004**, *20*, 7117; (e) Meldrum, F. C.; Kotov, N. A.; Fendler, J. H. *J. Phys. Chem.* **1994**, *98*, 4506; (f) Mayya, K. S.; Sastry, M. *J. Phys. Chem. B* **1997**, *101*, 9790; (g) Mayya, K. S.; Schoeler, B.; Caruso, F. *Adv. Funct. Mater.* **2003**, *13*, 183.

(4) (a) Drechsler, U.; Erdogan, B.; Rotello, V. M. *Chem. Eur. J.* **2004**, *10*, 5570; (b) Mirkin, C. A.; Letsinger, R. L.; Mucic, R. C.; Storhoff, J. J. *Nature* **1996**, *382*, 607; (c) Alivisatos, A. P.; Johnson, K. P.; Peng, X.; Wilson, T. E.; Loweth, C. J.; Bruchez, M. P., Jr.; Schultz, P. G. *Nature* **1996**, *382*, 609; (d) Storhoff, J. J.; Mucic, R. C.; Mirkin, C. A. *J. Cluster. Sci.* **1997**, *8*, 179; (e) Sastry, M.; Lala, N.; Patil, V.; Chavan, S. B.; Chittiboyina, A. G. *Langmuir* **1998**, *14*, 4138; (f) Shenton, W.; Davis, S. A.; Mann, S. *Adv. Mater.* **1999**, *11*, 449; (g) Fullam, S.; Rao, S. N.; Fitzmaurice, D. J. *Phys. Chem. B* **2000**, *104*, 6164; (h) Kumar, A.; Pattarkine, M.; Bhadbade, M.; Datar, S.; Dharmadhikari, C. V.; Ganesh, K. N.; Sastry, M. *Adv. Mater.* **2001**, *13*, 341; (i) Mandal, S.; Gole, A.; Lala, N.; Gonnade, R.; Ganvir, V.; Sastry, M. *Langmuir* **2001**, *17*, 6262; (j) Shipway, A. N.; Lahav, M.; Gabai, R.; Willner, I. *Langmuir* **2000**, *16*, 8789.

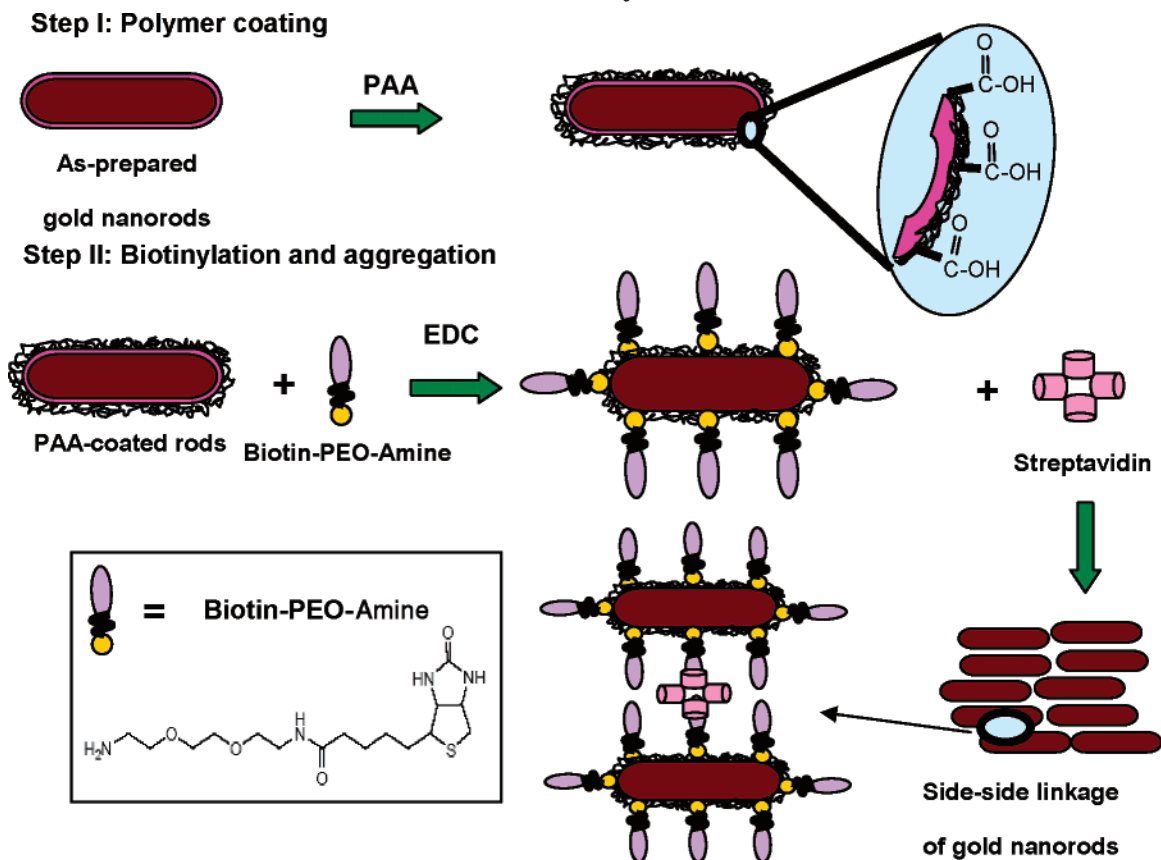
(5) (a) Kim, Y.; Johnson, R. C.; Hupp, J. T. *Nano Lett.* **2001**, *1*, 165; (b) Obare, S. O.; Hollowell, R. E.; Murphy, C. J. *Langmuir* **2002**, *18*, 10407.

(6) Templeton, A. C.; Wuelfing, W. P.; Murray, R. W. *Acc. Chem. Res.* **2000**, *33*, 27.

(7) (a) Rosi, N. L.; Mirkin, C. A. *Chem. Rev.* **2005**, *105*, 1547; (b) Thanh, N. T. K.; Rosenzweig, Z. *Anal. Chem.* **2002**, *74*, 1624.

(8) (a) Dujardin, E.; Hsin, L.-B.; Wang, C. R. C.; Mann, S. *Chem. Commun.* **2001**, 1264; (b) Mbindyo, J. K. N.; Reiss, B. D.; Martin, B. R.; Keating, C. D.; Natan, M. J.; Mallouk, T. E. *Adv. Mater.* **2001**, *13*, 249; (c) Chang, J.-Y.; Wu, H.; Chen, H.; Ling, Y.-C.; Tan, W. *Chem. Commun.* **2005**, *8*, 1092; (d) Caswell, K. K.; Wilson, J. N.; Bunz, U. H. F.; Murphy, C. J. *J. Am. Chem. Soc.* **2003**, *125*, 13914.

(9) (a) Thomas, K. G.; Barazzouk, S.; Ipe, B. I.; Joseph, S. T. S.; Kamat, P. V. *J. Phys. Chem. B* **2004**, *108*, 13066; (b) Nikoobakht, B.; Wang, Z. L.; El-Sayed, M. A. *J. Phys. Chem. B* **2000**, *104*, 8635; (c) Jana, N. R.; Gearheart, L. A.; Obare, S. O.; Johnson, C. J.; Edler, K. J.; Mann, S.; Murphy, C. J. *J. Mater. Chem.* **2002**, *12*, 2909; (d) Orendorff, C. J.; Hankins, P. L.; Murphy, C. J. *Langmuir* **2005**, *21*, 2022. (e) Chen, D.; Gao, L. *J. Cryst. Growth* **2004**, *264*, 216.

Scheme 1. Scheme Showing the General Methodology Used for Gold Nanorod Biotinylation and Subsequent 3-D Assembly.

biotin–streptavidin interaction for preferential end-to-end assembly of gold nanorods has been demonstrated by us.^{8d} There have also been reports which demonstrate the use of different weak interactions such as hydrogen bonding,^{9a} surfactant-mediated interactions,^{9b,c} electrostatic cross-linking,^{9d} and other secondary interactions^{9e} to form different solution-based assemblies and liquid-crystalline arrays of short and long inorganic nanorods.

In some of the reports mentioned above,⁸ bifunctional thiols have been used to modify the nanorod surface. In our case, the ends of gold nanorods display a {111} crystal face, and the side faces have {100} or {110} crystal structures.¹⁰ We and others have observed that thiols preferentially bind to the nanorod ends.^{8c,d,9a} Though this would be advantageous for certain applications, it would also be beneficial to have complete surface functionalization of nanorods.

In this report we demonstrate the biotinylation the gold nanorod surface. The as-prepared long gold nanorods (length ~ 600 nm, and thickness ~ 30 nm) are positively charged due to the presence of a bilayer of the capping surfactant cetyltrimethylammonium bromide (CTAB).^{3d,11,12c} This facilitates electrostatic adsorption of a carboxylic acid-containing polymer by the layer-by-layer approach.¹² As the polymer coats the entire gold nanorod surface, carboxylic acid groups are present over the entire nanorod surface. Next, a biotin molecule containing an amine group is anchored to the rods via the well-known carbodiimide chemistry. The resulting nanorods would

then, in principle, be uniformly biotinylated. Subsequent addition of streptavidin to these biotinylated gold nanorods leads to nanorod aggregation. A closer look at the aggregates reveals preferential side-to-side assembly of gold nanorods. The different steps involved in this process are shown in Scheme 1. The entire process was monitored by UV–vis spectroscopy, light scattering, and transmission electron microscopy measurements. Biotinylation of the nanorod ends^{8d} versus the entire nanorod surface is another step further toward achieving surface functionalization of gold nanorods.

Experimental Section

Materials. Chloroauric acid ($\text{HAuCl}_4 \cdot 3\text{H}_2\text{O}$), trisodium citrate, sodium borohydride (NaBH_4), ascorbic acid, and the polyelectrolyte poly(acrylic acid, sodium salt) (PAA), MW ~ 15000 g/mol, were all obtained from Aldrich and used as received. EZ-link biotin–PEO–amine, MW ~ 374.50 g/mol (spacer arm ~ 2 nm) and 1-ethyl-3-(3-dimethylaminopropyl) carbodiimide hydrochloride (EDC), MW ~ 191.7 g/mol, were purchased from Pierce Chemicals and used as received. Streptavidin (from *Streptomyces avidinii*), MW ~ 60 kDa, and cetyltrimethylammonium bromide (CTAB) were obtained from Sigma and used as received. Sodium chloride (NaCl) was purchased from Fisher. All glassware was cleaned with aqua regia and rinsed with deionized water prior to experiments. The water used for all experiments was Fisher-brand deionized ultrafiltered water.

Synthesis of Gold Nanorods. Gold nanorods were synthesized by the seed-mediated, template assisted protocol as has been described elaborately in our earlier publications.¹³ This protocol gives fairly monodisperse, stable gold nanorods (stabilized by a bilayer of CTAB)^{3d,12c,13} that have lengths ~ 500 –

(10) Jana, N. R.; Gearheart, L. A.; Obare, S. O.; Johnson, C. J.; Edler, K. J.; Mann, S.; Murphy, C. J. *J. Mater. Chem.* **2002**, *12*, 2909.

(11) Nikoobakht, B.; El-Sayed, M. A. *Langmuir* **2001**, *17*, 6368.

(12) (a) Decher, G. *Science* **1997**, *277*, 1232; (b) Gittins, D. I.; Caruso, F. *J. Phys. Chem. B* **2001**, *105*, 6846; (c) Gole, A.; Murphy, C. J. *Chem. Mater.* **2005**, *17*, 1325.

(13) (a) Jana, N. R.; Gearheart, L.; Murphy, C. J. *J. Phys. Chem. B* **2001**, *105*, 4065; (b) Gole, A.; Murphy, C. J. *Chem. Mater.* **2004**, *16*, 3633.

600 nm and diameters $\sim 25\text{--}30$ nm.^{3d,13} This protocol produces a high percentage of gold nanorods, although small rods and other shapes (triangles and spheres) are also present.^{13b}

Polyelectrolyte Coating of Gold Nanorods. Aliquots of as-prepared (un-purified, containing excess CTAB) gold nanorods were placed in 1.5-mL microcentrifuge tubes and centrifuged once at 8000 rpm for 6 min. A pellet of gold nanorods was formed at the bottom of the microcentrifuge tubes. The supernatant colorless solution (containing excess CTAB) was slowly removed without disturbing the pellet. For polyelectrolyte coating experiments, two pellets were combined to double the nanorod concentration.

Stock solutions of PAA at 10 mg/mL concentration were prepared in 1 mM aqueous NaCl solution. To the microcentrifuge tubes containing the gold nanorod pellets were added 1 mL of 1 mM NaCl aqueous solution and 200 μL of PAA stock solution. After 30-min adsorption time, the excess polymer in the supernatant fraction was removed by centrifuging and rinsing twice (7000 rpm, 6 min), and finally redispersing the pellet in 1 mL of deionized water. The coated nanorods were stable for weeks, as judged by the absence of any color change.

Biotinylation. A 10^{-4} M stock solution of EZ-link biotin-PEO-amine was prepared in deionized water and stored at 4 °C. A 10^{-2} M stock solution of EDC was prepared in deionized water and stored below 0 °C. Both these solutions were equilibrated to room temperature before use. To 1 mL of PAA-coated gold nanorod solution, 100 μL each of stock solution of biotin-PEO-amine and EDC were added stepwise under vigorous stirring. Stirring was continued for 10–20 s, and then the rods were stored undisturbed for a period of 24 h.

3-D Assembly of Nanorods. A 1.6×10^{-5} M stock solution of streptavidin was prepared in deionized water and stored below 0 °C. Before addition to biotinylated rods, the streptavidin solution was equilibrated to room temperature. To 1 mL of a solution of biotinylated rods, 20 μL of stock solution of streptavidin was added under vigorous stirring conditions. The solution was stirred for 1 min and stored at room temperature for further analysis.

Instrumentation. UV–vis spectroscopy was performed on a Varian model Cary 500 Scan UV–vis–NIR spectrophotometer. Light scattering and ζ -potential measurements were performed on a Brookhaven Zeta PALS instrument. Transmission electron microscopy (TEM) measurements were performed on a Hitachi H-8000 TEM instrument operating at an accelerating voltage of 200 kV. TEM samples were prepared by immersing the TEM grids (for 10 min) inside a vial containing 200 μL of nanorod solution which was to be analyzed. Subsequently the solution was removed after this period, and any small drops left on the TEM grid were removed using a tissue paper. This method is slightly different from the one we normally use to prepare TEM samples, wherein we dry a drop of nanorod solution onto a TEM grid for 1 h. Experimentally we observed a difference for these two approaches. When nanorods are dried on a TEM grid, they form specific patterns on the grid surface due to water evaporation;¹⁴ these patterns can be avoided by using the method used herein. The method used here was specifically used for our purpose in this report in order to rule out any evaporation-related arrangement of gold nanorods. TEM was also used to determine the separation distance between individual nanorods.

Control Experiments. TEM and light-scattering measurements were performed on as-prepared gold nanorods, gold nanorods after PAA coating, and after biotinylation (but without addition of streptavidin) to rule out any non-specific aggregation.

Results and Discussion

Biotinylation of nanoparticles is a key step in order to utilize them for bio-sensing applications.⁴ Usually, a biotin molecule with a thiol group at one end is used to modify inorganic nanoparticles because of the high affinity of thiols toward noble metals.^{4e–g,8d} Anisotropic nanocrystals, particularly gold nanorods, which we routinely synthesize in our laboratory,¹³ gave interesting biotinylation results.^{8d}

Biotin disulfide preferentially bound to the Au {111} faces of the gold nanorod ends.^{8d} Addition of streptavidin further led to the end-to-end assembly of large gold nanorods.^{8d} In this new study, to achieve entire surface biotinylation of gold nanorods, we had to couple two different techniques: (a) anionic polymer adsorption using a carboxylic acid-containing polymer (poly(acrylic acid), PAA) and (b) carbodiimide chemistry to link biotin-PEO-amine to the PAA layer.

Carbodiimide chemistry is commonly used to form amide bonds between carboxylic acids and primary amines. The carbodiimide 1-ethyl-3-(3-dimethylaminopropyl) carbodiimide hydrochloride (EDC) is used for this process. As a first step, EDC reacts with a carboxylic acid group and forms an amine-reactive intermediate. In the next step, addition of a primary amine-containing molecule in this reaction mixture leads to an amide linkage between the amine and the activated carboxylic acid group. The activation is generally done at low pH (pH ~ 4.5) because at this pH the acid is protonated. Biochemists use this procedure to link biomolecules or to modify biomolecule surfaces.¹⁵ Recently this technique has also been used to link antibodies and functional groups to inorganic nanoparticle surfaces and also for nanoparticle immobilization.¹⁶ These protocols involve surface modification of nanoparticles with bifunctional thiols followed by coupling of suitable analytes via EDC-mediated bond formation.¹⁶ In our case, removal of the bilayer of CTAB around the gold nanorods and further replacing it with thiol or amine molecules having a carboxylic acid functionality is a cumbersome process. Frequently, removal of CTAB leads to nanorod aggregation. Instead, the simple and versatile method of coating gold nanorods with polymers as previously demonstrated by us^{12c} has been used in part to first coat rods with suitable polymer exposing carboxylic acid groups, and later attach the amine group of the biotin-PEO-amine to its surface using carbodiimide chemistry. This has been shown in Scheme 2.

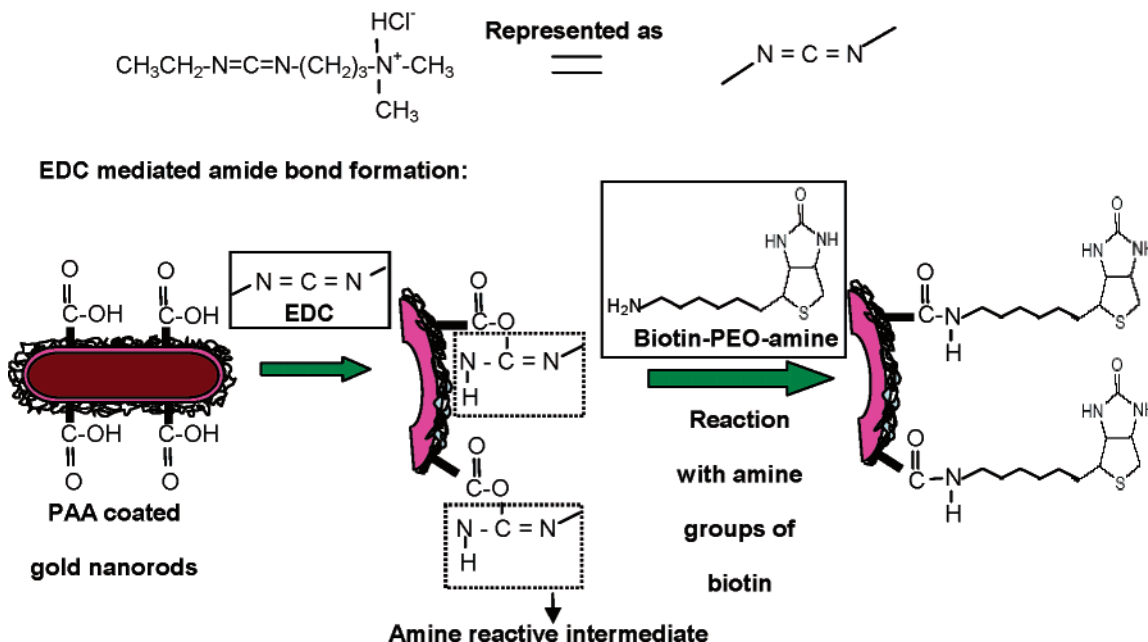
In our case, the choice of working pH was important to maintain the stability of gold nanorods. Light scattering and TEM analysis suggested a small amount of aggregation for nanorods biotinylated at pH ~ 4.5 , making it less advisable to work at that pH from a materials point of view (data not shown for brevity). A compromise was needed between the low pH requirement for EDC activation and nanorod aggregation. The beauty of using PAA is 2-fold. First, it has carboxylic acid groups which can be used for EDC-mediated amide bond formation with biotin-PEO-amine; second, because PAA is a weak polyelectrolyte, it has a pH-dependent ionization profile for the carboxylic acid moieties. The pH profile of the ζ -potential of the PAA-coated gold nanorods is shown in Figure 1. At low pH values, the ζ -potential of the gold nanorods is low because fewer of the carboxylic acid groups

(15) (a) Sivakumar, M.; Rao, K. P. *J. Biomat. Sci. Polym. Ed.* **2002**, *13*, 111; (b) Takeoka, Y.; Sasada, K.; Nishiwaki, Y.; Rikukawa, M.; Sanui, K. *Colloids Surf., A* **2005**, *257*, 485. (c) Kim, K.; Kwon, S.; Park, J. H.; Chung, H.; Jeong, S. Y.; Kwon, I. C.; Kim, I.-S. *Biomacromolecules* **2005**, *6*, 1154; (d) Gooding, J. J.; Praig, V. G.; Hall, E. A. H. *Anal. Chem.* **1998**, *70*, 2396; (e) Lee, J. B.; Kim, D.-J.; Choi, J.-W.; Koo, K.-K. *Colloids Surf., B* **2005**, *41*, 163.

(16) (a) Lee, J.; Govorov, A. O.; Dulka, J.; Kotov, N. A. *Nano Lett.* **2004**, *4*, 2323; (b) Mikhaylova, M.; Kim, D. K.; Berry, C. C.; Zagorodni, A.; Toprak, M.; Curtis, A. S. G.; Muhammed, M. *Chem. Mater.* **2004**, *16*, 2344; (c) Ozsoz, M.; Erdem, A.; Kerman, K.; Ozkan, D.; Tugrul, B.; Topcuoglu, N.; Ekren, H.; Taylan, M. *Anal. Chem.* **2003**, *75*, 2181; (d) Sheeney, H.-I. L.; Wasserman, J.; Willner, I. *Adv. Mater.* **2002**, *14*, 1323; (e) Shipway, A. N.; Lahav, M.; Gabai, R.; Willner, I. *Langmuir* **2000**, *16*, 8789.

(14) (a) Sau, T. K.; Murphy, C. J. *Langmuir* **2005**, *21*, 2923; (b) Nikoobakht, B.; Wang, Z. L.; El-Sayed, M. A. *J. Phys. Chem. B* **2000**, *104*, 8635; (c) Jana, N. R. *Angew. Chem., Int. Ed.* **2004**, *43*, 1536.

**Scheme 2. Scheme Showing EDC Chemistry for PAA-Coated Gold Nanorods
1-ethyl-3-(3-dimethylaminopropyl) carbodiimide hydrochloride (EDC)**



are deprotonated ($\text{pK}_a \sim 4.5$).^{17a} An increase in the pH of the gold nanorod solution leads to an increase in ζ -potential, due to an increase in the degree of ionization of the carboxylic acid groups of the PAA layer. This pH-dependent ionization behavior is typical of weak polyelectrolytes such as PAA (as opposed to strong polyelectrolytes such as polystyrenesulfonate, PSS). This has been observed previously by Caruso, Granick, and others.¹⁷ From Figure 1, it is clear that there are un-ionized

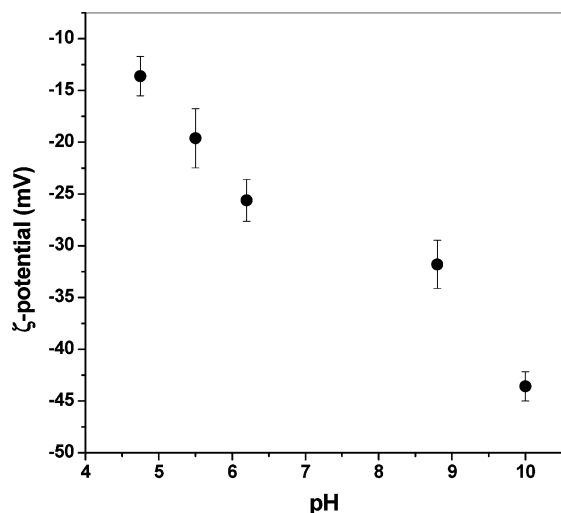


Figure 1. pH-dependent ζ -potential of PAA-coated gold nanorods.

carboxylic acid groups in the pH range of 5–6. This pH range is ideal for our studies, where we do not observe any pH-related aggregation; also, there is consistent biotinylation as observed by light-scattering studies. Hence, for all the experiments, a working pH ~ 5.5 was selected.

The polymer coating, biotinylation, and subsequent streptavidin-mediated aggregation have all been followed by UV-vis spectroscopy, as shown in Figure 2. The curves

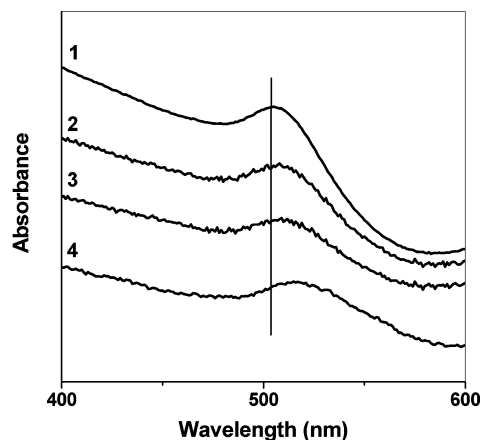


Figure 2. UV-vis spectra of gold nanorods at different stages of coating and aggregation. Curve 1: as-prepared purified gold nanorods; curve 2: gold nanorods after coating with a single layer of PAA; curve 3: PAA-coated gold nanorods after biotinylation; curve 4: biotinylated gold nanorods aged 1 h after addition of streptavidin. The spectra have been vertically shifted for clarity.

have been shifted vertically for clarity. As mentioned earlier, the gold nanorods were synthesized by our three-step seed-mediated protocol.¹³ This protocol gives fairly monodisperse gold nanorods with dimensions of 500–600-nm length and 25–30-nm thickness.¹³ Along with rods, a small percentage of short rods, triangles, and spheres are also produced which have absorbance in the 800–1200-nm range as observed by us previously.^{13b} To avoid interference of absorbance due to these secondary shapes and to analyze the wavelength shifts due to surface modification and aggregation solely for gold nanorods, we have primarily investigated the transverse plasmon band of the gold nanorod (400–600-nm region). We believe that significant plasmon band shifts can be seen in this region and could hence be attributed to nanorod surface modi-

(17) (a) Blaakmeer, J.; Bohmer, M. R.; Cohen Stuart, M. A.; Fleer, G. J. *Macromolecules* **1990**, *23*, 2301; (b) Kato, N.; Schuetz, P.; Fery, A.; Caruso, F. *Macromolecules* **2002**, *35*, 9780; (c) Xie, A. F.; Granick, S. *J. Am. Chem. Soc.* **2001**, *123*, 3175.

fication. Curve 1 (Figure 2) shows the spectra of the as-prepared purified (CTAB removed by centrifugation) gold nanorods. A transverse plasmon band can be clearly seen around 505 nm. Upon capping these gold nanorods by a single layer of PAA, there is a small shift in this band to 508 nm (curve 2, Figure 2). Such small shifts (~ 3 nm) in the plasmon bands have been previously observed independently by our and Caruso's group upon polymer coating.^{3g,12b,c} These shifts are due to the variation of local dielectric function of polymer-coated nanoparticles versus as-prepared nanoparticles. There is a small additional red-shift upon biotinylation (510 nm; curve 3, Figure 2). Addition of streptavidin dramatically red-shifts the plasmon band (517 nm; curve 4, Figure 2). This indicates aggregation of gold nanorods mediated by the protein molecules,^{2b,4} as confirmed by light scattering and TEM (see below).

Light scattering coupled with TEM measurements were used as a measure to determine aggregation, if any, of the gold nanorods at various stages of surface modification. Light scattering indicates the effective diameter of the as-prepared gold nanorods to be ~ 38 nm in solution, with a ζ -potential around +30 mV. The positive charge on the rods is due to the presence of a bilayer of CTAB.^{11,12c} It is important to note here that the size of the as-prepared gold nanorods (by TEM measurements) is ~ 600 nm in length and ~ 30 nm in thickness.¹³ On the other hand, light scattering typically shows an effective diameter of ~ 38 nm. The light-scattering analysis assumes that particles are spherical; hence, the actual sizes determined by light scattering in our case cannot be taken literally. Therefore we have used light-scattering measurements solely to monitor the aggregation kinetics of the gold nanorods, not to evaluate spatial parameters of the nanorods.

The effective diameter of the gold nanorods upon coating with a single layer of PAA reaches ~ 40 nm, and the ζ -potential changes to ~ -20 mV (at pH ~ 5.5). The negative ζ -potential shows successful coating of the gold nanorods by a layer of PAA. It is important to note here that a single layer of polystyrene sulfonate (PSS) around the gold nanorods results in a ζ -potential of more than -50 mV, as shown by us previously.^{12c} A lower ζ -potential in this case is due to a weaker polyelectrolyte (PAA) used here, which has a pH-dependent ζ -potential profile as shown in Figure 1. Upon biotinylation, the effective diameter of the gold nanorods reaches a value around 42 nm, and there is no significant change in the charge on the gold nanorods. TEM analysis of gold nanorods at different stages was also performed to rule out aggregation. These TEM micrographs have been displayed as Supporting Information: Figures S1 (as-prepared gold nanorods), S2 (PAA-coated gold nanorods), and S3 (biotinylated gold nanorods). In all these cases, the nanorods are well dispersed without any signs of aggregation. Hence, a smooth increase in the effective diameter of the gold nanorods observed by light-scattering measurements indicates an increase in the hydrodynamic radius of the particles due to adsorption of different surface modifiers and not the aggregation of the nanorods.

Light scattering was also used to study the streptavidin-mediated aggregation of gold nanorods. As mentioned in the Experimental Section, 20 μ L of 1.6×10^{-5} M stock solution of streptavidin was added to 1 mL of biotinylated gold nanorods, and the kinetics of aggregation were monitored by light scattering. It can be seen from Figure 3 (circles) that, as a function of time, the effective diameter of the gold nanorods rapidly increases and reaches a stable value. This rapid increase in the size of the nanorods

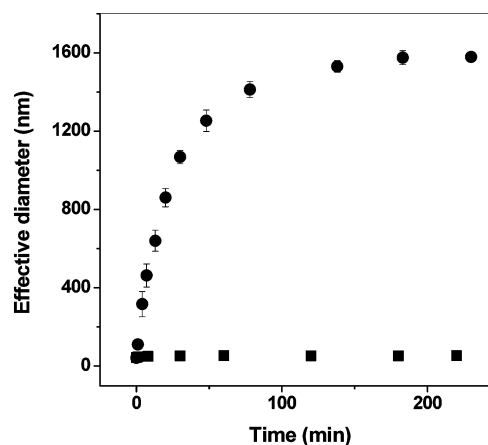


Figure 3. Light-scattering aggregation kinetics of gold nanorods as a function of time after the addition of streptavidin. Circles: PAA-coated gold nanorods + biotin + EDC; squares: PAA-coated gold nanorods + biotin (no EDC added).

indicates the formation of a 3-D assembly, as confirmed by TEM measurements (explained later). As explained earlier, the actual data values in this curve cannot be taken literally with regard to the correct sizes of gold nanorods (initial effective diameter by light scattering ~ 40 nm, initial nanorod size by TEM measurements ~ 600 nm length, and thickness ~ 30 nm). Hence, the nature of the curve observed and the time required for saturation of the kinetics are the only two factors that would be meaningful in this case. A better parameter that could be considered here is the effective increase in the size of the aggregate upon addition of streptavidin. Simple calculations on the light-scattering data suggest roughly a 3-fold increase in the size of the nanorod assembly in the first minute after addition of streptavidin and about a 30-fold increase in less than an hour. The growth saturates in about little more than an hour with the aggregate being about 36-fold bigger than the individual gold nanorod. This corresponds to a size of individual aggregate to be roughly of the order of about 4μ m. Such large aggregates have been confirmed by TEM measurements (as shown later).

A control experiment was performed wherein 100 μ L of stock solution of biotin-PEO-amine was added to 1 mL of PAA-coated gold nanorods. This time, EDC was not added to the reaction mixture. After storing these rods for 24 h as in other cases, 20 μ L of streptavidin was added to 1 mL of this reaction mixture, and any possible aggregation was monitored by light-scattering measurements. No aggregation of the gold nanorods due to biotin-streptavidin interaction is observed. These data are shown in Figure 3 (squares). This clearly demonstrates the role played by EDC in biotinylating the PAA-coated gold nanorods. Furthermore, this also indicates that a mere electrostatic bond which the amine groups of the biotin-PEO-amine molecules might possibly form with the deprotonated carboxylic acid groups of the PAA layer is not stable enough to promote streptavidin-mediated nanorod aggregation. It is essential to have a strong amide linkage between the biotin and the PAA layer to facilitate streptavidin-directed 3-D assembly.

TEM measurements were performed on the gold nanorods upon addition of streptavidin to visualize the nature of the aggregates. Figure 4, parts A-F, shows the TEM micrographs of the aggregated gold nanorods at different magnifications. As mentioned in the Experimental Section, TEM samples were prepared by immersing the TEM grids in nanorod solutions for 10 min and then draining the

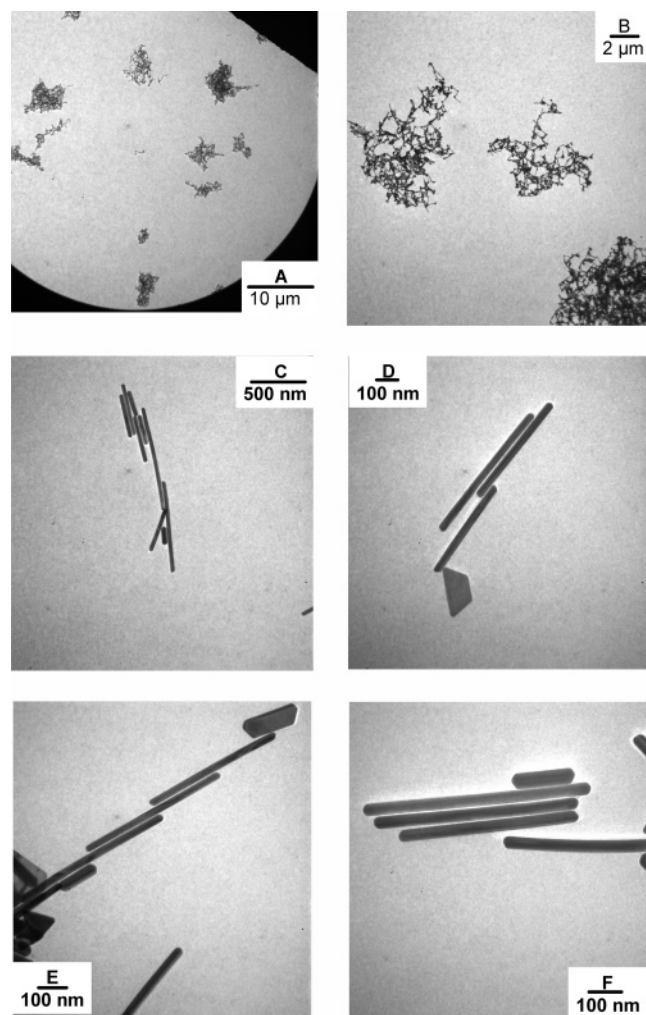


Figure 4. TEM micrographs of streptavidin-mediated 3-D assembly of biotinylated gold nanorods at different magnifications.

excess solution. This method was used (instead of drying nanorod drop onto TEM grids) to rule out any water-evaporation-induced arrangement of gold nanorods. All the samples for TEM were prepared after 1 h of addition of streptavidin to the biotinylated gold nanorods. The low-magnification images (Figure 4, parts A and B) clearly display large aggregates roughly of the size 2–4 μm . This size agrees well with the light-scattering data discussed previously. Zooming in different regions of such aggregates reveals a general trend of side-to-side aggregation of gold nanorods. This can be clearly seen in micrographs of Figure 4, parts C–F. All these micrographs were recorded from different regions of the TEM grid to confirm uniformity of the side-to-side linkages. The reproducibility of such side-to-side linkages was confirmed by repeatedly checking the entire process by TEM measurements. It is interesting to note that the nanorods are not “aggregated” like one would observe in a typical salt-induced aggregation, but

there is a well-defined separation between such cross-linked nanorods. This distance was found to be $\sim 6.5 \pm 0.8$ nm after inspecting different micrographs of high magnification. This distance coincides with the size of a typical streptavidin molecule (~ 4 nm) plus the length of the biotin spacer arm (~ 2 nm). This clearly suggests that the gold nanorods are aggregated by streptavidin molecules.

The TEM micrographs at different stages of surface modification and aggregation were analyzed, and parameters such as the number of nanorods assembled side-to-side and end-to-end, the number of individual nanorods, and distances between the linked rods were calculated. This is displayed in Table 1. For each case, around five micrographs recorded in different regions of the TEM grid were studied, and the results were averaged. It can be clearly seen that for the as-prepared, PAA-coated, and biotinylated gold nanorods (first 3 rows, Table 1) there is a high percentage of unlinked (random) rods and a small percent of assembled nanorods either in the side–side or end–end fashion. The distances between the gold nanorods assembled side–side were measured. Nanorods separated more than one nanorod diameters (>30 nm) were not included for analysis because we believe that there might be no interactions whatsoever between the nanorods at such distances and could, for all practical purposes, be considered as randomly distributed nanorods. We would like to point out that the distances observed between linked nanorods here are higher than that observed earlier.^{14a} This might be due to the method used for TEM sample preparation (drying sample versus removal of excess sample by suction, as used here). The concentration of gold nanorods in that case was significantly higher than that in the case reported herein, leading to concentration-dependent clustering of gold nanorods upon drying. It is interesting to note that upon PAA coating, the distance between the gold nanorods decreases. This might possibly be due to hydrogen bonding between the protonated carboxylic acid groups on the nanorod surface. Moreover, the important point to be noted in this analysis is that the distances between the assembled rods in the first three rows of Table 1 are quite different from what one would observe in a typical biotin–streptavidin aggregate (row 4, Table 1). This clearly supports the concept that streptavidin cross-links the biotinylated gold nanorods and supports the aggregation studies.

Conclusions

In this report we have demonstrated a biotin–streptavidin-mediated aggregation of gold nanorods. In one of our previous publications, we had demonstrated an end-to-end linkage of gold nanorods mediated by biotin–streptavidin interaction.^{8d} The disulfide biotin used in that case could modify the gold nanorod ends and leave the side faces as-is. Coating the gold nanorods with a layer of PAA and subsequently attaching biotin–PEO–amine to the carboxylic acid groups of the PAA layer using carbodiimide chemistry helps to biotinylate the entire

Table 1. Parameters Obtained from the Analysis of TEM Images

system	side–side assembly of nanorods (%)	end–end assembly of nanorods (%)	random nanorods (unlinked) (%)	rod–rod distances ^a (for side–side assembled nanorods) (nm)
as-prepared gold nanorods	16.3 ± 15.3	10.2 ± 3.4	72.6 ± 10.5	18.7 ± 5.7 nm
PAA-coated gold nanorods	31.2 ± 12.8	13.3 ± 5.6	56.4 ± 10.6	3.5 ± 2.4 nm
biotinylated gold nanorods	35.3 ± 16.6	16.8 ± 5.8	48.1 ± 7.0	16.3 ± 4.8 nm
biotin–streptavidin reaction (aggregated gold nanorods)	58.7 ± 2.9	24.3 ± 5.6	17.1 ± 2.8	6.5 ± 0.8 nm

^a Nanorods separated more than one nanorod diameters (>30 nm) were not included for analysis.

nanorod surface. Subsequent addition of streptavidin leads to the aggregation of gold nanorods. These aggregated nanorods show a general trend of side–side linkage with separation distances comparable to the bridging streptavidin molecule. This aggregation has been confirmed by light scattering and TEM measurements. Such entire surface biotinylation of gold nanorods could be useful for different sensing applications. Attaching nanoparticles, proteins, viruses, and so forth, to the gold nanorod surface, either on the nanorod ends or on the entire surface via specific interactions, is an interesting possibility and is currently being pursued in our laboratory.

Acknowledgment. We thank the National Science Foundation and the University of South Carolina for funding.

Supporting Information Available: TEM micrographs of as-prepared gold nanorods (S1), gold nanorods coated with a single layer of PAA (S2), and biotinylated gold nanorods (S3). This material is available free of charge via the Internet at <http://pubs.acs.org>.

LA0512704